CO_2/CH_4 Separation by Facilitated Transport in Amine-Polyethylene Glycol Mixtures

Richard A. Davis and Orville C. Sandall
Dept. of Chemical and Nuclear Engineering, University of California, Santa Barbara, CA 93106

In this work, the separation of carbon dioxide from methane by reactive liquid membranes consisting of the secondary amines, diethanolamine, and diisopropanolamine in polyethylene glycol with an average molecular weight of 400 was studied. A mathematical model was developed to describe the transport process. This model employs the zwitterion mechanism for the CO_2 amine reaction kinetics. Membrane flux experiments utilizing a flat plate device were carried out to verify the model predictions. It was found that large permeabilities and separations were achieved for low CO_2 feed concentrations. The results also show that DEA based solutions give better separation than DIPA based solutions.

Introduction

Large quantities of methane are generated by the decomposition of biological and industrial waste. A key to the recovery of a gas with a high heating value is an efficient means of separating the methane from its primary diluent, carbon dioxide (Ashare, 1981; Zimmerman et al., 1985). In addition, synthetic natural gas produced from coal or low grade natural gases generally contains large concentrations of carbon dioxide, CO_2. The traditional means of purifying such fuel gases are scrubbing with either a physical solvent or a chemically reactive solution in which acid gases such as CO_2 and H_2S are preferentially absorbed (Astarita et al., 1983), and preferential adsorption, for example, on activated charcoal (Kohl and Riesenfeld, 1985). Recently, however, increasing attention has been focused on membrane-based processes because of their compactness, simple modular construction, and energy savings (Kulkarni et al., 1983; Schell, 1985; Baker and Blume, 1986).

In this research, the separation of CO_2 from CH_4 is studied using a supported liquid membrane. Selectivity for CO_2 is enhanced by the choice of a solvent having favorable differences in solubility and diffusivity between the two gases and through the addition of a nonvolatile reactant to the liquid phase. Primary and secondary amines have been applied extensively in industrial scrubbing processes for CO_2, and they are used here as the reactant component. Meldon et al. (1986) demonstrated good selectivity plus high absolute permeability for CO_2 in polyethylene glycol/amine films immobilized in the micropores of polypropylene membranes.

The amine/solvent mixture examined in this study was selected on the basis of the following criteria. The solvent needs to be compatible with the liquid support, must be one in which CO_2 is highly soluble and preferably one in which CH_4 is less so. In addition, the solvent must be comparatively nonvolatile (as measured by a high boiling point) and be miscible with the amine. A solvent with low volatility is needed in order to maintain membranes having a long life. The amine must also be nonvolatile and react reversibly with CO_2.

On this basis, experiments were conducted with diethanolamine (DEA) and polyethylene glycol (PEG) in view of prior experience with this mixture in membrane studies (Meldon and Nair, 1986). DEA is a secondary amine that is widely used in industry for chemical scrubbing because of its favorable reaction kinetics in aqueous solutions. DEA also exhibits a high degree of stability. Additional experiments were carried out with another promising secondary amine, diisopropanolamine (DIPA). In this work, a model is developed to describe this transport process and controlled experiments were carried out to test model predictions. The results of this study will facilitate rationalization of the earlier results of Meldon and Nair (1986) and suggest operating regimes for further investigation.

Transport Mechanism

Figure 1 depicts the transport of gas A due to "facilitated transport" or "carrier-mediated transport." Gas A dissolves

---

Correspondence concerning this article should be addressed to O. C. Sandall.

Current address of R. A. Davis: Dept. of Chemical Engineering, University of Minnesota, Duluth, MN 55812.

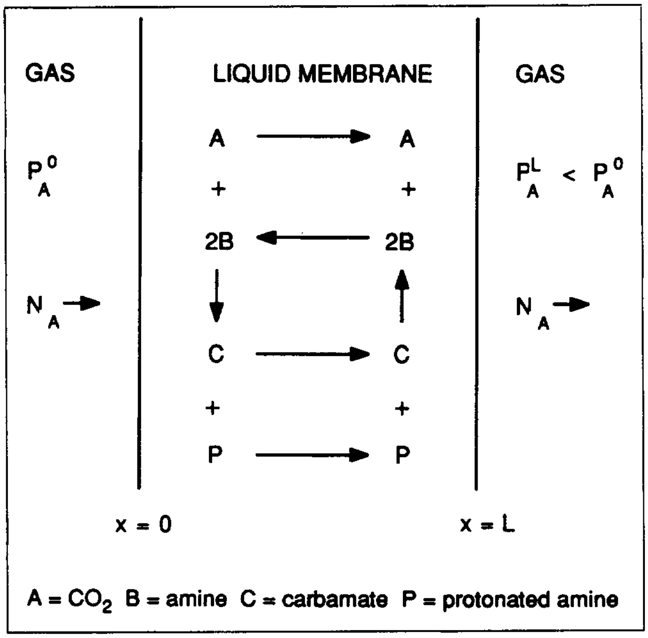

Figure 1. Diffusion and reaction of CO_2 across an immobilized liquid membrane of a secondary amine, DEA or DIPA, in PEG-400.

into the liquid film at the high pressure boundary and reacts with reactant B. The flux of solute gas A from the high to low partial pressure sides of the membrane is enhanced by the additional flux of reaction products, as shown in this figure. At the low partial pressure side of the film the reaction is reversed and the solute is released to desorb from the liquid where it is swept away by a receiving gas and the carrier species recycles back to the high pressure side of the membrane.

Reversible Reaction Kinetics

The reaction between CO_2 and secondary amines produces a protonated amine and a carbamate species. The overall reaction is:

$$CO_2 + 2R_2NH \rightleftharpoons R_2NH_2^+ + R_2NCO_2^- \tag{1}$$

where R represents the functional groups on the amine. There has been considerable debate about the reaction mechanism. The order of reaction with respect to the amine has been reported to range from one to two. Danckwerts (1979) proposed a zwitterion mechanism which appears to explain the discrepancy in the reported order of reaction. This mechanism involves two steps. Initially, CO_2 reacts with the amine to form the reactive intermediate zwitterion. In the second step, the proton is removed from the zwitterion by a second amine molecule to form the products carbamate and a protonated amine.

$$CO_2 + R_2NH \underset{k_2}{\overset{k_1}{\rightleftharpoons}} R_2NH^+CO_2^- \tag{2}$$

$$R_2NH^+CO_2^- + R_2NH \underset{k_4}{\overset{k_3}{\rightleftharpoons}} R_2NCO_2^- + R_2NH_2^+ \tag{3}$$

Note that in nonaqueous solvents, only the amine deprotonates the zwitterion in the second step. Application of the steady-state approximation to the zwitterion gives the following rate expression for the forward rate of reaction of CO_2

$$r_{CO_2} = \frac{\left\{C_A C_B - \dfrac{C_C C_P}{K C_B}\right\}}{\left\{\dfrac{1}{k_1} + \dfrac{k_2}{k_1 k_3}\dfrac{1}{C_B}\right\}} \tag{4}$$

where A, B, C and P represent CO_2, amine, carbamate and protonated amine respectively and C_j is the concentration of species j. The equilibrium constant, K, is defined here as the ratio of the forward rate constants to the reverse rate constants as

$$K = \frac{k_1 k_3}{k_2 k_4} \tag{5}$$

Versteeg et al. (1989) have shown that the zwitterion mechanism successfully describes the experimental results for this reaction reported in the literature. The rate expression in Eq. 4 is used in the model developed in the next section for facilitated transport of CO_2 by the species DEA and DIPA.

Model Development

The flux of CO_2 across the liquid membrane can be modeled by simple mass balances for each component. The model is for membranes with a flat plane geometry. Thus, the transport is assumed to be one-dimensional in the direction perpendicular to the membrane surface, as shown in Figure 1. The local steady-state species balances are of the form:

$$-\frac{dN_i}{dx} = r_i \tag{6}$$

where N_i represents the flux of species i and x is the coordinate in the direction perpendicular to the membrane surface. The flux of species i in a liquid is generally described by Fick's Law:

$$N_i = x_i(N_i + N_j) - D_j\frac{dC_j}{dx} \tag{7}$$

where x_i, C_i and D_i are the mole fraction, concentration and diffusion coefficient, respectively, of component i in liquid j. The first term represents the contribution to the flux from bulk flow motion of the liquid. This term is neglected because x_i is small and the liquid phase is considered stationary. Thus, the transport is by diffusion alone. In the case of the ionic product species, a third term accounting for electrical effects is sometimes added to the righthand side of Eq. 6. However, in this model, the diffusivities of all the amine species are assumed to be equal. Several methods for estimating diffusivity are empirical modifications of the Stokes-Einstein equation. The diffusion coefficients are found to depend on the ratio of the square root of the solute molecular weight and the molar volume of the solute at the normal boiling point raised to the $-1/3$ or $-2/3$ power (Reid et al., 1986). Table 1 compares the molecular

Table 1. Comparison of Molecular Weight and Molar Volume for DEA, Protonated DEA and Carbamate

Molecular Species	$\sqrt{MW}$ $(g/mol)^{1/2}$	Molar Vol.* $V_B^{-1/3}$ $(mol/cm^3)^{1/3}$ Schroeder	Le Bas	Molar Vol. $V_B^{-2/3}$ $(mol/cm^3)^{2/3}$ Schroeder	Le Bas
		DEA			
R_2NH	10.27	0.20	0.20	0.040	0.040
$R_2NCO_2^-$	12.17	0.19	0.19	0.037	0.035
$R_2NH_2^+$	10.30	0.20	0.20	0.038	0.039
		DIPA			
R_2NH	11.54	0.19	0.19	0.037	0.037
$R_2NCO_2^-$	13.27	0.19	0.18	0.035	0.033
$R_2NH_2^+$	11.58	0.19	0.19	0.036	0.036

* Estimations by additive volume methods of Schroeder and Le Bas (Reid et al., 1986).

weights and approximate molar volumes of the three amine species for DEA and DIPA. The relative differences in properties of these molecules are small indicating that the diffusivity of these molecules may be approximated as equal. Hence, in the absence of imposed external electric fields, the local electroneutrality condition must be satisfied as follows:

$$C_p - C_C = 0 \tag{8}$$

Thus, assuming constant diffusivity with respect to position, the species balance equations are reduced to:

$$D_i \frac{dC_i^2}{dx^2} = r_i \quad (i = A, B, C) \tag{9}$$

subject to the following boundary conditions:

$$C_A = \begin{cases} C_A^0 = \dfrac{P_A^0}{H_A} & \text{at } x = 0 \\ C_A^L = \dfrac{P_A^L}{H_A} & \text{at } x = L \end{cases} \tag{10}$$

$$\frac{dC_i}{dx} = 0 \text{ at } x = 0, L \ (i \neq A) \tag{11}$$

where H_A represents Henry's constant for the solubility of CO_2 in the liquid solvent. The former boundary conditions assume equilibrium between the gas and liquid phases at the interface. The nonvolatile species are confined to the liquid phase. Hence, the flux of the amine based species vanishes at the gas/liquid boundaries.

As demonstrated by Goddard et al. (1970), the boundary conditions are not independent. An additional constraint is necessary to completely specify the problem. Because the net reaction rate is zero, the global concentration of the amine based species is constant. By assuming the diffusion coefficients are equal the conservation of amine takes the form:

$$C_B + C_C + C_P = C_B^i \tag{12}$$

Equations 8 and 12 combined with the species balance equations eliminates C_C and C_P. The reaction rate expression in Eq. 4 for components A and B becomes:

$$r_A = \frac{1}{2} r_B = \frac{\left\{ C_A C_B - \dfrac{(C_B^i - C_B)^2}{4KC_B} \right\}}{\left\{ \dfrac{1}{k_1} + \dfrac{k_2}{k_1 k_3} \dfrac{1}{C_B} \right\}} \tag{13}$$

The retention of C_B instead of C_C or C_P is only a matter of convenience in the model solution procedure.

Model Solution

The solution of the model equations is conveniently represented in terms of the facilitation factor which is the ratio of the enhanced flux with reaction to the flux without reaction.

$$\psi = \frac{\left. \dfrac{dC_A}{dx} \right|_{x=0}}{\left(\dfrac{C_A^L - C_A^0}{L} \right)} - 1 = \frac{dA}{dz} \left(\frac{C_A^0}{C_A^L - C_A^0} \right) - 1 \tag{14}$$

The facilitation factor, ψ, is defined as the increased dimensionless flux of the dissolving species due to the chemical reaction.

The solution to the model equations involves solving a system of nonlinear stiff second-order differential equations. Several approximate solutions have been developed for limiting cases—of facilitated transport (Smith et al., 1973; Suchdeo and Schultz, 1974). Numerical solutions are necessary when the solution lies between these limits.

Equilibrium limit

The upper limit on the facilitation factor is where the reaction reaches equilibrium everywhere in the liquid film (Smith et al., 1973; Goddard et al., 1970). The equilibrium limit involves very fast reactions or thick membranes such that the ratio of the reaction time to diffusion time is small. These films are characterized by a large Damköhler number, δ. The solution procedure for the equilibrium facilitation factor involves integrating the total flux equation assuming the reaction is at equilibrium and evaluating the result at the membrane boundaries. The reacting species are constrained to be at equilibrium. The equilibrium facilitation factor for this case is:

$$\psi_{eq} = \frac{D_B C_B^i \sqrt{K}}{D_A (\sqrt{C_A^0} - \sqrt{C_A^L})(1 + 2\sqrt{KC_A^0})(1 + 2\sqrt{KC_A^L})} \tag{15}$$

In dimensionless form, assuming negligible CO_2 at the low partial pressure boundary ($C_A^L = 0$), the equilibrium facilitation factor is simply

$$\psi_{eq} = \frac{\alpha\sqrt{\gamma}}{1 + 2\sqrt{\gamma}} \tag{16}$$

where

$$\gamma = KC_A^0, \text{ and } \alpha = \frac{D_B C_B^i}{D_A C_A^0}.$$

Goddard et al. (1970) have rigorously shown that Eq. 27 is the upper bound on the facilitation factor.

Numerical solution

The model equations can only be solved exactly by numerical methods. Because of the stiffness of the solution, creative solution procedures have been developed to capture the rapidly changing solution near the liquid membrane gas-liquid interface.

Finite difference techniques are attractive for stiff problems. However, the differential equations are nonlinear requiring iterative trial and error solution techniques. Convergence is slow for poor initial guesses. Computation is also intensive due to the large numbers of divisions required to capture the effects in the reaction boundary layers. Nedelman and Rubinow (1981) employed a finite difference technique in conjunction with a nonuniform mesh size to investigate the facilitated diffusion of oxygen and carbon monoxide. Again, good initial guesses were required to achieve convergence. An alternative numerical technique which proved to be amenable to this problem is the method of quasilinearization in conjunction with a finite-difference solution (Kutchai et al., 1970).

The flux of solute into the liquid is directly proportional to the gradient of the solute in the liquid at the gas-liquid interface. In problems of this nature, the reaction boundary layer contains the steeper gradients. In this work, an improvement to the solution method avoids the large number of steps by judiciously placing small increments in regions of large gradients and large increments where the solution is relatively "flat." This was accomplished by solving the problem initially with equal divisions then searching for the regions of large gradients by approximating the derivative numerically.

Sasidhar and Ruckenstein (1983) used a relaxation method in the case of large Damköhler numbers to avoid the necessity of good initial guesses. However, this technique converges slowly to the steady-state solution. In the present technique, the numerical solutions for small Damköhler numbers were used as initial guesses for solutions involving large Damköhler numbers. A computer program has been developed to perform these tasks automatically.

Liquid Membrane Properties

Several key properties were determined experimentally in order to implement the model. The details of these experiments have been reported elsewhere (Davis, 1992; Davis et al., 1993; Davis and Sandall, 1993). In all cases data were obtained for the temperature range of 20-40°C over a concentration range of 0-30 wt. % DEA and DIPA. The results were correlated for temperature and concentration dependence and are summarized here for convenience.

Gas solubility

The solubility of CO_2 in amine-PEG solutions was correlated for temperature and concentration dependence by the semiempirical equation in the form of the Clausius-Clapayron equation

$$\ln H_A = h_1 + \frac{h_2}{R_g T} \tag{17}$$

where $R_g = 8.314$ kJ/(kmol·K) is the ideal gas constant. The composition dependence for DEA is found in the following correlations:

$$h_{1,\mathrm{DEA}} = 7.036 + 0.1633w - 0.004365w^2 \tag{18}$$

$$h_{2,\mathrm{DEA}} = -14.26 - 0.3655w + 0.01246w^2 \tag{19}$$

For DIPA solutions, the composition terms are:

$$h_{1,\mathrm{DIPA}} = 7.036 - 0.01981w + 0.001686w^2 \tag{20}$$

$$h_{2,\mathrm{DIPA}} = -14.26 + 0.06722w - 0.002095w^2 \tag{21}$$

Chemical equilibrium

The experimental results for the equilibrium constants for the overall reaction of CO_2 with the secondary amines were correlated by the Gibbs-Helmholtz equation. For DEA-PEG solutions

$$\ln K_{\mathrm{DEA}} = -20.68 + \frac{65{,}980}{R_g T} \tag{22}$$

The results for DIPA solutions were correlated to give:

$$\ln K_{\mathrm{DIPA}} = -14.99 + \frac{50{,}580}{R_g T} \tag{23}$$

Diffusivity

The experimental results for the diffusivity of CO_2 in the amine-PEG solutions were correlated by the following functional form proposed by Akgermann and Gainer (1972) for small molecules diffusing through a medium consisting of much larger molecules

$$\ln D_A = d_1 + \frac{d_2}{R_g T} \tag{24}$$

where the DEA composition dependence is correlated as:

$$d_{1,\mathrm{DEA}} = -21.40 - 0.01983w - 0.001453w^2 \tag{25}$$

$$d_{2,\mathrm{DEA}} = 4{,}618 + 41.92w + 2.676w^2 \tag{26}$$

The DIPA diffusivity composition dependent terms are:

$$d_{1,\mathrm{DIPA}} = -21.40 + 0.1200w - 0.009203w^2 \tag{27}$$

$$d_{2,\mathrm{DIPA}} = 4{,}618 - 281.7w + 21.76w^2 \tag{28}$$

The diffusivity of the amine species in amine-PEG mixtures was estimated from a modified Stokes-Einstein relationship for viscous liquids (Cussler, 1984) using data from Hikita et al. (1980) for aqueous amine solutions.

$$\frac{D_B}{D_B^o} = \left(\frac{\eta}{\eta^o}\right)^{-2/3} \tag{29}$$

where the superscript o indicates properties in aqueous solutions. The dynamic viscosity of water was taken from Reid et al. (1976):

$$\log \eta^o (cP) = -1.5668 + \frac{230.298}{T - 146.797} \tag{30}$$

The diffusivity for the amines in water was estimated from the correlation of Hikita et al. (1980)

$$\left(\frac{D_B^o \eta^o}{T}\right) = 2.5 \times 10^{-10} \left(\frac{\text{cm}^2 \cdot \text{poise}}{\text{s} \cdot \text{K}}\right) \tag{31}$$

Liquid viscosity

The dynamic viscosity results for the amine-PEG solutions were correlated for temperature and concentration dependence according to the following modified Andrade expression:

$$\ln \eta = n_1 + \frac{n_2}{T} + n_3 T \tag{32}$$

where for DEA solutions:

$$n_{1,\text{DEA}} = -45.14 - 0.9828w + 0.02040w^2 \tag{33}$$

$$n_{2,\text{DEA}} = 9{,}061 + 167.9w + 3.219w^2 \tag{34}$$

$$n_{3,\text{DEA}} = 0.04934 + 0.001437w - 3.143 \times 10^{-5} w^2 \tag{35}$$

In the case of DIPA-PEG, the correlation of the dynamic viscosity data gives:

$$n_{1,\text{DIPA}} = -45.14 - 1.243w + 0.02879w^2 \tag{36}$$

$$n_{2,\text{DIPA}} = 9{,}061 + 210.3w - 4.280w^2 \tag{37}$$

$$n_{3,\text{DIPA}} = 0.04934 + 0.001819w - 4.727 \times 10^{-5} w^2 \tag{38}$$

Reaction rate constants

The experimental results for the reaction rate constants were correlated for temperature dependence by an Arrhenius expression. The results for the CO_2-DEA reaction kinetics in PEG are:

$$k_{1,\text{DEA}} = 7.996 \times 10^{12} \exp\left(\frac{-57{,}470}{R_g T}\right) \tag{39}$$

$$\left(\frac{k_1 k_3}{k_2}\right)_{\text{DEA}} = 2.519 \times 10^{14} \exp\left(\frac{-57{,}470}{R_g T}\right) \tag{40}$$

The DIPA kinetic results were correlated for the following expressions:

$$k_{1,\text{DIPA}} = 5.400 \times 10^{12} \exp\left(\frac{-57{,}470}{R_g T}\right) \tag{41}$$

$$\left(\frac{k_1 k_3}{k_2}\right)_{\text{DIPA}} = 3.443 \times 10^{13} \exp\left(\frac{-57{,}470}{R_g T}\right) \tag{42}$$

Flux Measurements

Experiments designed to measure the flux of N_2O, CO_2, and CH_4 through liquid membranes composed of DEA and DIPA in PEG-400 were conducted to verify the model predictions for CO_2 transport. The liquid was supported by flat sheets of polypropylene membranes. A flow cell technique was employed for these experiments. Initially, the flux of the nonreactive N_2O was measured to determine the effective membrane thickness. Then, the flux of CO_2 and CH_4 was measured to obtain experimental values for the facilitation and separation factors.

Liquid supports

The most common method for preparing experimental liquid membranes is to impregnate the pores of a porous polymer membrane with the solvent-carrier solution. By soaking a polymeric membrane in the solvent, thin liquid films have been generated. Polycarbonate membrane filters are attractive because they have uniform straight-through pores and the diffusional path length and porosity are well known from microscopy techniques. However, it was found in the case of polycarbonate that the PEG-400 dissolved the membrane material. Polypropylene membranes were used here because of their chemical compatibility with PEG and the amines and their large relative porosity. The disadvantage with this material is that the pores are not uniform and follow a tortuous path through the membrane. Therefore, diffusion experiments were necessary to determine the effective pore length in the polypropylene membranes.

Flow cell technique

A flow cell apparatus similar to the design of Bateman et al. (1984) was constructed to experimentally verify the mathematical model of CO_2 transport through the reactive liquid membrane. A schematic of the apparatus is shown in Figure 2. A polymeric flat sheet membrane is housed in a cell designed to allow a feed stream and a sweep gas to pass on opposite sides of the membrane. The polymer membrane is sandwiched between two Plexiglass plates. Polypropylene screens fill the spaces between the membrane and the plate to support the

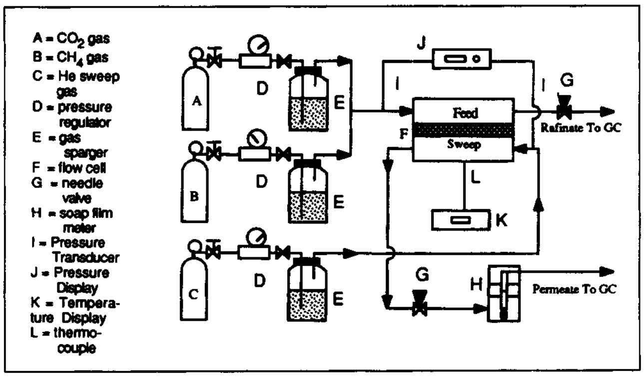

Figure 2. Membrane gas separation apparatus.

membrane. Teflon gaskets were placed between the plates and the membrane on each side to prevent the gases from leaking and to act as spacers for the gas flow paths. The total exposed area on each surface of the membrane was 232 cm^2. The gas streams were introduced evenly across one end of the cell and collected at the other end through a row of small ports drilled into the plates. The cell was held together with 16 bolts spaced evenly around the edge of the plates. The feed stream, consisting of methane and CO_2, and the sweep stream, consisting of helium or nitrogen, was saturated with the solvent before passing to the cell in order to avoid any evaporation of the liquid from the pores of the membrane. The gas flow rates were controlled with needle valves and measured with a soap film meter. The pressures of the gas streams were controlled with pressure regulators. The gas inlet and exit compositions were determined by gas chromatography. The experimental flux of solute through the membrane is calculated as the molar flow rate divided by the surface area of the membrane as follows:

$$N_i = \frac{P_i V_G}{R_g T A_m} \tag{43}$$

where P_i is the partial pressure of gas i in the permeate stream, V_G is the volumetric gas flow rate and A_m is the exposed polymer membrane surface area. The molar flow rate is calculated assuming the gas behaves ideally under the operating conditions of the experiment.

The procedure consisted of setting the gas feed flow rate such that the partial pressure of CO_2 remained constant. The sweep stream flow rate was also set to keep the partial pressure of CO_2 in the permeate relatively small ($<1\%$ of feed composition). Once the flow rates were set, the compositions of the gas streams were determined by gas chromatography. In this manner, the partial pressure gradient of CO_2 across the membrane was taken as the partial pressure of CO_2 in the feed stream. The composition of the sweep stream was monitored for several minutes to insure that steady-state operation was achieved before data were collected to determine the permeability of the gas.

Membrane tortuosity and porosity

In the case of polypropylene membranes, the pores take a tortuous path through the membrane. Thus, the effective diffusional path length for the solute gases is greater than the physical polymer membrane thickness. In the experimental flux expression, the increased length is accounted for in the tortuosity factor, τ, defined as the ratio of the diffusional path length to the nominal film thickness. An additional correction is applied to the flux expression for the volume occupied by the supporting material. The membrane porosity, ϵ, is defined as the ratio of the liquid volume in the pores to the nominal membrane volume. Now, the facilitation factor is related to the experimental flux based on the exposed membrane surface area as:

$$N_i = \frac{(\psi + 1) D_i \Delta P_i \epsilon}{N_i L \tau} \tag{44}$$

where ΔP_i is the partial pressure difference of species i at the membrane surfaces and L is the membrane thickness. For a nonreacting gas such as N_2O, the facilitation factor goes to zero and the ratio of the porosity to tortuosity can be determined from flux measurements through a supported liquid membrane. The permeability, Q_i, is determined by rearranging Eq. 44 for the ratio of the enhancement factor multiplied by the diffusion coefficient to the Henry's Law constant. This gives:

Table 2. Tortuosity Factors for Celgard 2500 Polypropylene Membranes Impregnated with Amine/PEG-400 Solutions at $T = 24°C$ and $\Delta P = 1.0$ atm

wt. %	DEA	DIPA
0	2.3	2.3
10.0	2.1	2.4
20.0	1.9	2.2
30.0	2.0	1.8
Average	2.1	2.2

$$Q_i = \frac{(\psi + 1) D_i}{H_i} = \frac{N_i L \tau}{\Delta P_i \epsilon} \tag{45}$$

The experimental flux term is measured according to Eq. 43. Permeabilities are commonly reported in Barrer units [1 Barrer = 1 cm^3(STP)·cm/(cm^2·s·cmHg·10^{10})]. Experiments were performed to obtain permeabilities for a range of amine concentrations at low and high partial pressures of CO_2.

Initial flux measurements were performed with N_2O in the amine/PEG-400 solvents to determine the tortuosity in the liquid support. The results from these experiments were necessary to interpret the flux measurements of CO_2 and CH_4 in the reactive amine/PEG-400 solutions.

Tortuosity factor

Celgard 2500 hydrophobic polypropylene membranes were used in this work to support the liquid. The manufacturer specifies the porosity of the dry membrane material as 0.45 with an effective pore size of 0.04 μm. The membrane is manufactured to a thickness of 25 ± 2.5 microns. The results for tortuosity using the manufacturers porosity are listed in Table 2. Several experimental values for tortuosity are available in the literature. Wolf and Strieder (1990) give a value from a theoretical study in which the microporous membrane is modeled as overlapping fibers. All these values are given in Table 3 for comparison. The results found in this investigation are

Table 3. Tortuosity Factors for Celgard 2500 Polypropylene Membranes from the Literature

Immobilized Liquid	Solute	τ	Reference
Xylene	Acetic Acid	2.47	Prasad et al. (1986)
Methyl Isobutyl Ketone	Acetic Acid	2.03	Prasad et al. (1986)
Water	N_2	2.23	Bhave and Sirkar (1986)
Formamide	NO	2.0	Bateman et al. (1984)
Theoretical	—	1.8	Wolf and Strieder (1990)

Table 4. Permeability of CO_2 and CH_4 in DEA/PEG-400 Solutions at $T=24°C$ and $\Delta P=1$ atm

wt. %	Q_{CO_2} (Barrer)[2] 100% P Exp./Model	 0.5% P Exp./Model	Q_{CH_4}	High P $\frac{Q_{CO_2}}{Q_{CH_4}}$	Low P $\frac{Q_{CO_2}}{Q_{CH_4}}$
0	730/810	730/810	390	1.9	1.9
10.0	550/610	10,000/9,200	320	1.7	34
20.0	450/480	11,000/12,000	300	1.5	37
30.0	360/400	9,000/9,500	210	1.7	43

in agreement with tortuosities reported in the literature when the literature values, including the prediction of Wolf and Strieder (1990), are averaged. Thus, the average value of $\tau = 2.1$ was used in the calculations for permeability and in the model predictions.

Permeability coefficients

Experiments were done to obtain the permeabilities of CO_2 and CH_4 in DEA/PEG-400 and DIPA/PEG-400 solutions for 0-30 wt. % amine. The experimental results and model predictions for permeability are given in Tables 4-5. All the flux measurements were performed at room temperature. The partial pressures of CO_2 in the feed stream were fixed at 1 and 0.005 atm. The choice of pressures was based on predictions for the facilitation factor from the diffusion-reaction model. At pressures lower than ~0.005 atm, the assumption of negligible CO_2 in the permeate breaks down for the experimental conditions. The estimated experimental error in the permeability results is ±12%. The maximum estimated error in the model predictions due to uncertainties in the model parameters for the permeability is ±15%. As shown in Figures 3-6, the model predicts the experimental results for permeability within the estimated errors. In the case of $P_{CO_2} = 1.0$ atm, the model predictions are consistently higher than the experimental results as seen in Figures 3 and 4. This may be the effect of the change in the liquid properties due to the high solubility and reaction of CO_2 to form the ionic product species which was not accounted for in the model predictions. This may be explained in terms of the ionic effects due to the presence of relatively large concentrations of the products species in the liquid. The ionic effects are twofold. First, the increased ionic concentration may increase the liquid viscosity and hence cause the diffusivity of the solutes species to decrease. Secondly, there may be an ionic "salting out" effect causing the solubility of the dissolving gases in the liquid to decrease. In the case of low CO_2 partial pressure in the feed, the effect of low concentrations of ions relative to the unreacted amine would be small. Although the experimental correlations for the necessary parameters do not strictly apply to the case where there are large concentrations of carbamate and protonated amine in the liquid, the more interesting and useful results were found to be for the situation of low feed CO_2 partial pressures where ionic effects may be neglected. The separation factors in the case of low feed CO_2 partial pressure are plotted in Figure 7. There are three significant observations which stand out from these results. First, the permeability of CO_2 is larger in DEA solutions. Second, the permeability reaches a maximum value then decreases as the amine concentration increases. This is

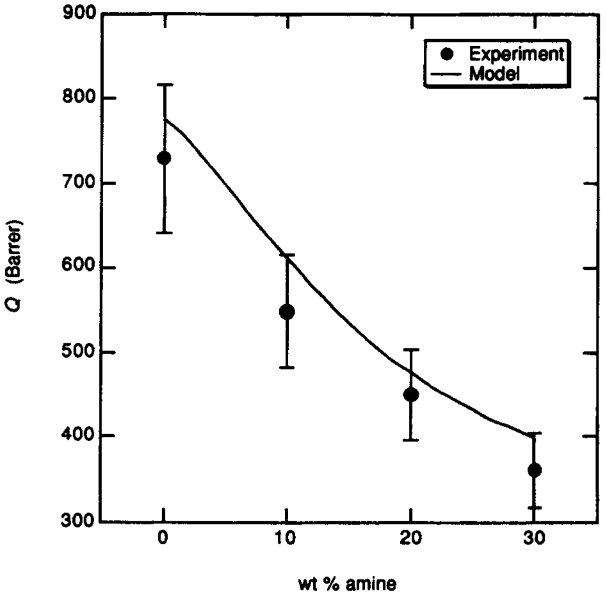

Figure 3. Q vs. DEA solvent composition: $P_{CO_2} = 1$ atm, $T=24°C$.

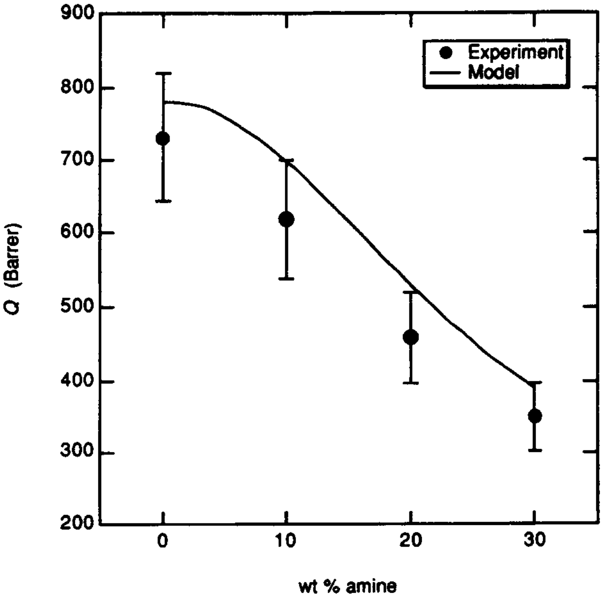

Figure 4. Q vs. DIPA solvent composition: $P_{CO_2} = 1$ atm, $T=24°C$.

Table 5. Permeability of CO_2 and CH_4 in DIPA/PEG-400 Solutions at $T=24°C$ and $\Delta P=1$ atm

wt. %	Q_{CO_2} (Barrer)* 100% P Exp./Model	 0.5% P Exp./Model	Q_{CH_4}	High P $\frac{Q_{CO_2}}{Q_{CH_4}}$	Low P $\frac{Q_{CO_2}}{Q_{CH_4}}$
0	730/810	730/810	390	1.9	1.9
10.0	620/700	8,400/7,100	330	1.9	26
20.0	460/530	8,700/9,000	310	1.5	28
30.0	350/390	6,700/7,100	220	1.6	30

* Permeability reported in Barrer units. 1 Barrer = 10^{-10} cm^3 (STP)·cm/cm^2-cm Hg·s

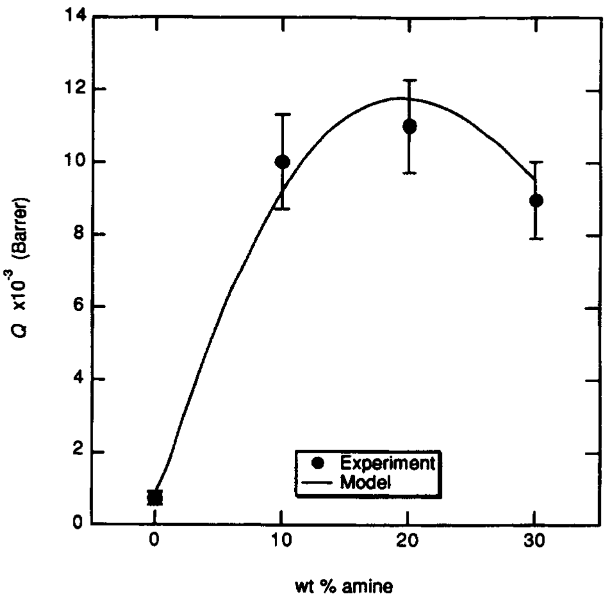

Figure 5. Q vs. DEA composition: $P_{CO_2} = 0.005$ atm, $T = 24°C$.

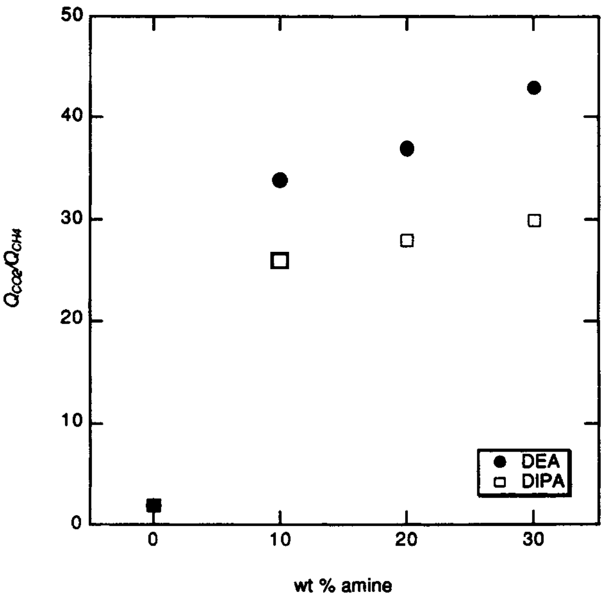

Figure 7. Separation factors for $P_{CO_2} = 0.005$ atm, $T = 24°C$.

most likely due to the lower diffusion coefficients for the more concentrated solutions. The third observation is that the permeability is much larger for the case of low partial pressure gradients across the membrane.

Parametric Study

The effects of CO_2 partial pressure, membrane thickness, composition and temperature on CO_2 transport through the liquid membrane are investigated with the aid of the diffusion-reaction model.

CO_2 partial pressure

It is apparent from the flux experiments and model predictions that the flux of CO_2 through the membrane is greatly enhanced for low CO_2 partial pressures in the feed gas. This is demonstrated dramatically by comparing the CO_2 concentration profiles in Figure 8 for 20 wt. % DEA in PEG at $P = 1$ and 0.005 atm, respectively. Note that the flux is directly proportional to the concentration gradient at the gas-liquid interface. Model predictions for the facilitation factor as a function of CO_2 partial pressure are shown in Figure 9. These results show that the facilitation improves gradually with lower pressures then increases sharply for partial pressures below ~ 0.1 atm. Thus, there appears to be a small range of conditions where the CO_2 transport is in transition from small to large facilitation. This corresponds to $\gamma \sim 10$ for this work. This result is in agreement with a study by Kemena et al. (1983)

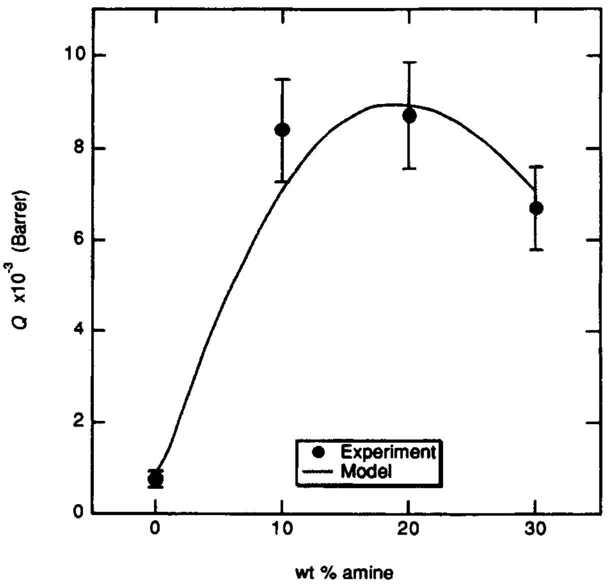

Figure 6. Q vs. DIPA composition: $P_{CO_2} = 0.05$ atm, $T = 24°C$.

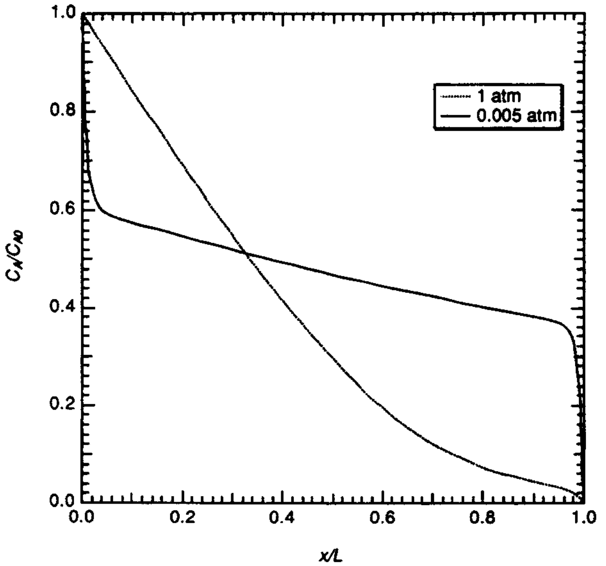

Figure 8. Dimensionless concentration profiles for CO_2 in 20 wt. % DEA.

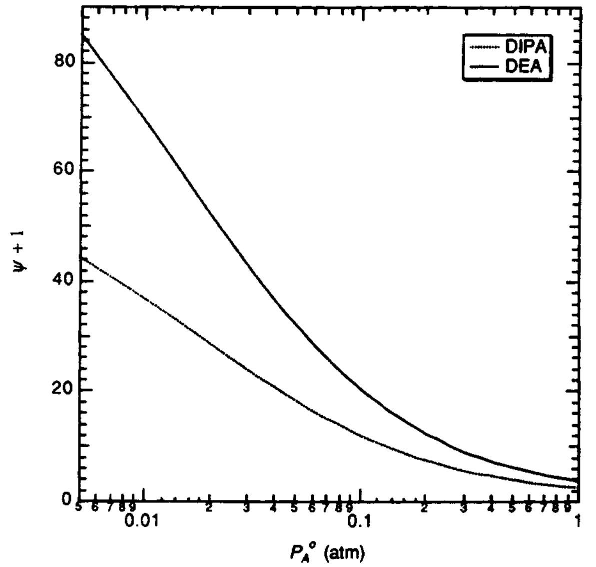

Figure 9. ψ vs. P_A^o (at $x=0$) for the facilitated transport of CO_2 in DEA/PEG-400 and DIPA/PEG-400 at $T=24°C$.

who reported the optimum range of γ to be 1 to 10 over a wide range of operating conditions. As expected, the concentration and reaction rate profiles become symmetric when γ falls below 10.

Damköhler numbers

The facilitation factor approaches the upper equilibrium limit for large Damköhler number. The Damköhler number, δ, is defined as:

$$\delta = \frac{L^2 k_1 C_B^i}{D_A} \tag{46}$$

This upper limit is demonstrated in Figures 10 and 11 for the experimental conditions of the flux measurements. The upper bound on the facilitation factor from Eq. 16 is given in Tables 6 and 7. In all cases there is practically no improvement in facilitation for Damköhler numbers greater than 10^{10}. The facilitation factor increases as the liquid membrane amine concentration increases due to the additional carrier available in the liquid phase.

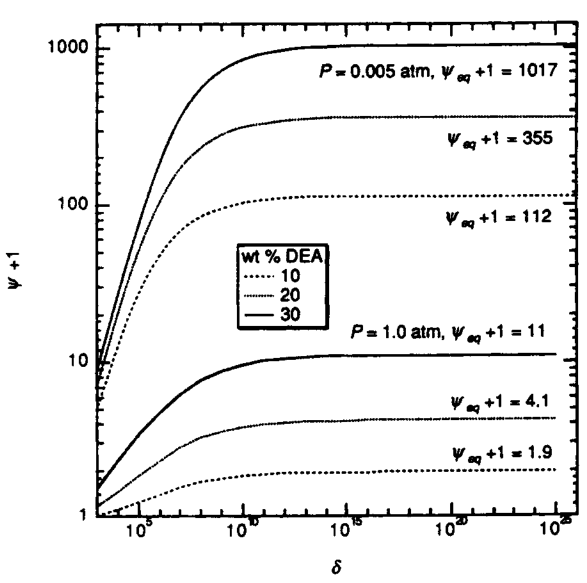

Figure 10. ψ vs. δ for CO_2 in DEA/PEG-400.

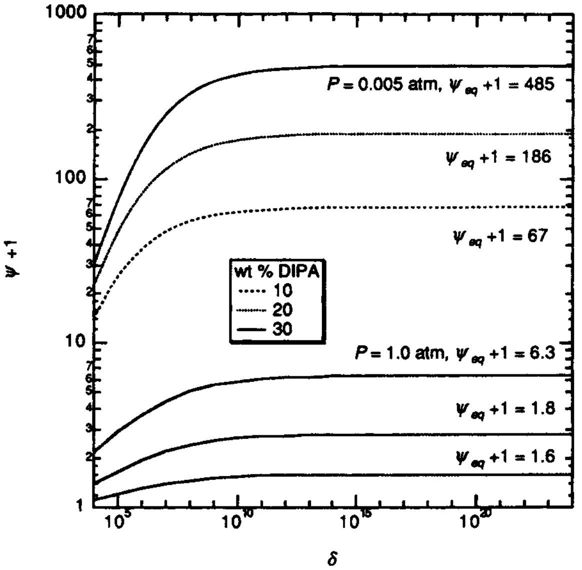

Figure 11. ψ vs. δ for CO_2 in DIPA/PEG-400.

Composition and temperature effects

There is an interesting result for the permeability as a function of initial amine composition. As was found above, the facilitation increases with amine concentration. However, the permeability for low CO_2 partial pressures reaches a maximum near 20 wt. % amine, as illustrated in Figures 5 and 6. This is due to the decreased diffusivity and solubility of CO_2 in the liquid. In the case of high CO_2 partial pressures at ambient temperature, the permeability decreases with increasing initial amine concentration and there is no advantage to using a reactive solvent. At higher temperatures, there appears to be a moderate amount of enhanced transport for the DIPA based solvent. The effects of temperature are also demonstrated in Figure 12 for 20 wt. % amine. As the temperature increases, the permeability increases because the diffusivity and the reaction rate increases. There is no permeability maximum with temperature for the range of the experimental parameters measured in this work.

Facilitation vs. separation factors

This research is intended to develop an effective liquid membrane process to separate CO_2 from CH_4. Such a process is characterized by a large CO_2 flux through the membrane in conjunction with large CO_2/CH_4 separation factors. The factors which affect the flux are the permeability, the partial pressure difference of CO_2 across the membrane and the membrane thickness. Note that the permeability is a function of the membrane thickness as well. The facilitation factor, and hence the permeability, increases while the total CO_2 flux decreases with

Table 6. Dimensionless Parameters for CO_2 Transport in DEA/PEG-400. $P^o_{CO_2} = 1$ and 0.005 atm, $T = 24°C$

ΔP (atm)	w	α	β	γ	δ	ψ	ψ_{eq}	Q (Barrer)
1	10	1.914	2.066	93.86	23,160	0.14	0.91	610
1	20	6.619	1.036	65.67	62,360	0.71	3.12	480
1	30	21.50	0.6923	40.12	141.900	2.57	9.96	400
0.005	10	382.9	2.066	0.4693	23,160	16.09	110.67	9,200
0.005	20	1,324	1.036	0.3284	62,360	41.17	353.54	12,000
0.005	30	4,300	0.6923	0.2006	141,900	84.17	1,015.9	9,500

a growing membrane thickness. Thus, it is not simply a matter of decreasing the membrane thickness to improve the flux of the permeate. There is a subtle compromise between shortening the diffusional path length and the additional carrier-mediated transport of the permeating species. One noted advantage of reactive liquid membranes over solid membranes is that relatively small membrane thicknesses are not required to achieve the same flux due to the additional carrier-mediated transport.

Conclusions

The conclusion based on the results of this study are summarized here. The main objective of this research was to characterize a liquid membrane based process for separating CO_2 from CH_4. A particular problem with liquid membranes is that there is solvent loss by evaporation. In this work the solvent PEG-400 which has a relatively low vapor pressure was chosen to increase the longevity of the liquid membrane. Two secondary amines, DEA and DIPA were added to the solvent in order to improve the selectivity of the membrane for CO_2 over CH_4. The results indicate that DEA/PEG-400 solutions achieved slightly higher permeabilities and better separation of CO_2 than DIPA based solutions. However, there is evidence which suggests that DIPA is less subject to deactivation by reaction with other contaminants such as carbonyl sulfide (COS) commonly present in methane based fuels (Kohl and Riesenfeld, 1985). The zwitterion mechanism proposed by Danckwerts (1979) was used to interpret the kinetics of the CO_2/secondary amine reaction. A mathematical model of the membrane transport process was developed which requires no adjustable parameters. Experiments were performed to determine the thermodynamic and transport properties of CO_2 in the liquid system which are required of the model. The N_2O analogy was employed to approximate these properties in cases where the CO_2/amine reaction interfered with direct measurements. Finally, the fluxes of CO_2 and CH_4 through the liquid membrane were measured in order to confirm the model predictions. Effective CO_2 permeabilities as high as 2,300 ± 12% Barrer and separation factors exceeding 40 were measured in the case of low CO_2 partial pressure in the feed gas. These results compare favorably with permeabilities and separation factors of 8 Barrer and 25, respectively reported for cellulose acetate polymer membranes operating under similar conditions (Perry and Green, 1986). At higher CO_2 partial pressures, there was little or no enhancement to the flux in the reactive liquid membranes. Hence, these amine/PEG liquid systems would be appropriate as a second step in a hybrid system where the bulk of the CO_2 is removed in the first step. Another application of this process is the case of upgrading biogas produced from landfills where methane is typically generated at atmospheric pressure.

It was found that the model predictions for the permeability of CO_2 in the liquid membranes agree with experiments within the estimated error bounds of the flux measurements. The information necessary for optimizing the conditions for CO_2/CH_4 separation has been determined thereby permitting the

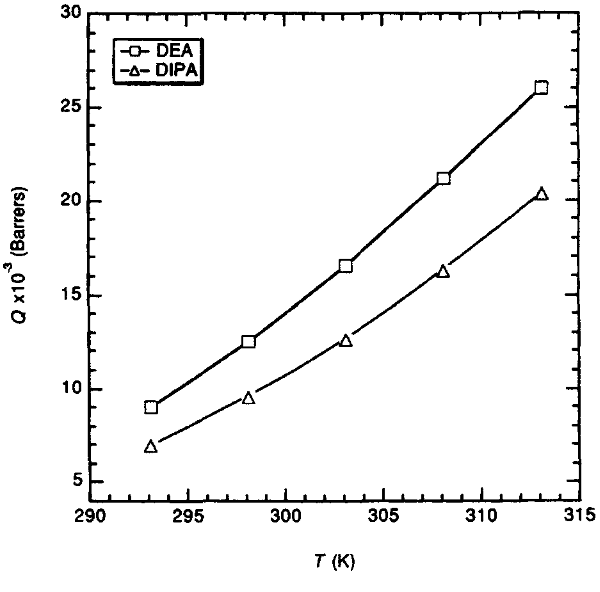

Figure 12. Q vs. T for CO_2 in 20 wt. % amine/PEG-400: $P^o_{CO_2} = 0.005$ atm.

Table 7. Dimensionless Parameters for CO_2 Transport in DIPA/PEG-400. $P^o_{CO_2} = 1$ and 0.005 atm, $T = 24°C$

ΔP (atm)	w	α	β	γ	δ	ψ	ψ_{eq}	Q (Barrer)
1.0	10.0	1.265	1.226	58.08	5,245	0.09	0.59	700
1.0	20.0	3.866	0.6204	41.95	12,830	0.41	1.79	530
1.0	30.0	11.60	0.4184	25.62	27,270	1.44	5.28	390
0.005	10.0	253.1	1.226	0.2904	5,245	10.00	65.64	7,100
0.005	20.0	773.3	0.6204	0.2097	12,830	22.91	184.83	9,000
0.005	30.0	2,320.0	0.4184	0.1281	27,270	43.27	483.94	7,100

rational design of a liquid membrane based process employing the liquid systems from this investigation.

Notation

A = dimensionless carbon dioxide concentration
A_m = membrane surface area, cm^2
B = dimensionless nonvolatile amine carrier concentration
C_i = concentration of species i, $kmol/m^3$
D_i = diffusion coefficient, cm^2/s
H_i = Henry's constant of species i, $atm \cdot m^3/kmol$
K = equilibrium constant, $m^3/kmol$
k_1, k_2, k_3, k_4 = kinetic rate constants, $m^3/(kmol \cdot s)$ or $1/s$
L = membrane thickness, m
N_i = flux of species i, $kmol/(m^2 \cdot s)$
P_i = partial pressure of species i, atm
Q = permeability, Barrer
r_i = reaction rate of species i, $kmol/(m^3 \cdot s)$
r_i^* = dimensionless reaction rate of species i
R = functional group on the amine
R_g = ideal gas constant, 82.05 $cm^3 \cdot atm/(mol \cdot K)$ or 8.314 $J/mol \cdot K$
T = absolute temperature, K
w = wt. % of the amine ion the solvent
x = distance into membrane, m
z = dimensionless length
V_G = gas volumetric flow rate, cm^3/s

Greek letters

α = separation factor or ratio of mobilities
β = dimensionless rate constant $= k_2/k_3 C_B^i$
δ = Damköhler number
ϵ = substrate porosity
γ = dimensionless equilibrium constant
η = dynamic viscosity, poise
τ = tortuosity factor of dimensionless time
ψ = facilitation factor

Subscripts

A = CO_2
B = R_2NH
C = $R_2NCO_2^-$
eq = equilibrium condition
P = protonated amine, $R_2NH_2^+$
Z = zwitterion, $R_2NH^+CO_2^-$

Superscripts

0 = at $x = 0$
o = pure solvent
i = initial concentration
L = at $x = L$

Literature Cited

Akgerman, A., and J. L. Gainer, "Diffusion of Gases in Liquids," *Ind. Eng. Chem. Fund.*, **11**, 373 (1972).

Ashare, E., "Analysis of Systems for Purification of Fuel Gas," *Fuel Gas Production From Biomass*, **Vol. II**, D. S. Wise, ed., CRC Press, Boca Raton, 1 (1981).

Astarita, G., D. W. Savage, and A. Bisio, *Gas Treating with Chemical Solvents*, McGraw-Hill, New York, 1 (1983).

Baker, R. B., and I. Blume, "Permselective Membranes Separate Gases," *Chemtech*, **16**, 232 (1986).

Bateman, B. R., J. D. Way, and K. M. Larson, "An Apparatus for the Measurement of Gas Fluxes through Immobilized Liquid Membranes," *Separ. Sci. Technol.*, **19**, 21 (1984).

Bhave, R. R., and K. K. Sirkar, "Gas Permeation and Separation by Aqueous Membranes Immobilized Across the Whole Thickness and Within a Thin Section of Hydrophobic Microporous Celgard Films," *J. Memb. Sci.*, **27**, 41 (1986).

Cussler, E., *Diffusion, Mass Transfer in Fluid Systems*, Cambridge University Press, New York (1984).

Davis, R. A., "The Separation of Carbon Dioxide from Methane by Facilitated Transport in Liquid Membranes," PhD Diss., University of California, Santa Barbara (1992).

Davis, R. A., and O. C. Sandall, "The Reaction of Carbon Dioxide with Secondary Amines in Polyethylene Glycol," *Chem. Eng. Sci.*, submitted for publication (1992).

Davis, R. A., R. E. Menéndez, and O. C. Sandall, "Physical, Thermodynamic and Transport Properties for Carbon Dioxide and Nitrous Oxide in Solutions of Diethanolamine or Diisopropanolamine in Polyethylene Glycol," *J. Chem. Eng. Data*, submitted for publication (1992).

Danckwerts, P. V., "The Reaction of CO2 with Ethanolamines," *Chem. Eng. Sci.*, **34**, 443 (1979).

Goddard, J. D., J. S. Scultz, and R. J. Bassett, "On Membrane Diffusion with Near-Equilibrium Reaction," *Chem. Eng. Sci.*, **25**, 665 (1970).

Guha, A. K., S. Majumdar, and K. K. Sirkar, "Facilitated Transport of CO_2 Through an Immobilized Liquid Membrane of Aqueous Diethanolamine," *Ind. Eng. Chem. Res.*, **29**, 2093 (1990).

Hikita, H., H. Ishikawa, K. Uku, and T. Murakami, "Diffusivities of Mono-, Di-, and Triethanolamine in Aqueous Solutions," *J. Chem. Eng. Data*, **24**, 324 (1980).

Kemena, L. L., R. D. Noble, and N. J. Kemp, "Optimal Regimes of Facilitated Transport," *J. Mem. Sci.*, **15**, 259 (1983).

Kohl, A. L., and F. C. Riesenfeld, *Gas Purification*, 3rd ed., Gulf Publishing Co., Houston (1979).

Kulkarni, S. S., E. W. Funk, N. N. Li, and R. L. Riley, "Membrane Separation Processes for Acid Gases," *AIChE Symp. Ser.*, **79**, 172 (1983).

Kutchai, H., J. A. Jacquez, and F. J. Mather, "Nonequilibrium-Facilitated Oxygen Transport in Hemoglobin Solution," *Bioph. J.*, **10**, 38 (1970).

Meldon, J. H., A. Paboojian, and G. Rajangam, "Selective CO_2 Permeation in Immobilized Liquid Membranes," *AIChE Symp. Ser.*, **82**, 114 (1986).

Meldon, J. H., and G. M. Nair, "Methane Carbon Dioxide Separation via Fractional Membrane Permeation," Paper 140f, AIChE Annual Convention, Miami Beach (Nov. 1986).

Nedelman, J., and S. I. Rubinow, "Facilitated Diffusion of Oxygen and Carbon Monoxide in the Large Affinity Region," *J. Math. Biol.*, **12**, 73 (1981).

Perry, R. H., and D. W. Green, *Perry's Chemical Engineers Handbook*, 6th ed., McGraw-Hill, New York (1986).

Prasad, R., A. Kiani, R. R. Bhave, and K. K. Sirkar, "Further Studies on Solvent Extraction with Immobilized Interfaces in a Microporous Hydrophobic Membrane," *J. Membrane Sci.*, **26**, 79 (1986).

Reid, R. C., J. M. Prausnitz, and B. E. Poling, *The Properties of Gases and Liquids*, McGraw-Hill, New York (1986).

Sasidhar, V., and E. Ruckenstein, "Relaxation Method for Facilitation Transport," *J. Mem. Sci.*, **13**, 67 (1983).

Schell, W. J., "Commercial Applications for Gas Permeation Membrane Systems," *J. Memb. Sci.*, **22**, 217 (1985).

Smith, K. A., J. H. Meldon, and C. K. Colton, "An Analysis of Carrier-Facilitated Transport," *AIChE J.*, **19**, 102 (1973).

Suchdeo, S. R., and J. S. Shultz, "The Permeability of Gases Through Reacting Solutions: the Carbon Dioxide-Bicarbonate Membrane System," *Chem. Eng. Sci.*, **28**, 13 (1974).

Versteeg, G. F., and W. P. M. van Swaaij, "On the Kinetics Between CO_2 and Alkanolamines Both in Aqueous and Non-Aqueous Solutions," *Chem. Eng. Sci.*, **43**, 573 (1988).

Wolf, J. R., and W. Strieder, "Surface and Void Tortuosities for a Random Fiber Bed: Overlapping, Parallel Cylinders of Several Radii," *J. Mem. Sci.*, **49**, 103 (1990).

Zimmerman, R. E., J. J. Walsh, and M. Wilkey, "Landfill Gas: Resource Evaluation and Development," Final rep., cont. 5083-224-0989, Gas Res. Institute, Chicago (1985).

Manuscript received Aug. 4, 1992, and revision received Dec. 3, 1992.